Capacity analysis for compact MIMO systems

Lau, Buon Kiong; Ow, Serene S. M.; Kristensson, Gerhard; Molisch, Andreas

Capacity Analysis for Compact MIMO Systems

B. K. Lau, S. M. S. Ow, G. Kristensson
Department of Electroscience,
Lund University, Sweden.
{Buon-Kiong.Lau@es, e00so@efd,
Gerhard.Kristensson@es}.lth.se

A. F. Molisch
Mitsubishi Electric Research Labs,
Cambridge, USA.

Department of Electroscience,
Lund University, Sweden.
Andreas.Molisch@ieee.org

Abstract—**We analyze the impact of mutual coupling on the capacity of MIMO systems with compact antenna arrays. Existing studies present conflicting views on the effect of mutual coupling. This is, in part, due to their different scopes and underlying assumptions of the system setups. In this paper, we aim to give a comprehensive picture by first examining the impact of mutual coupling on three capacity-related performance measures: antenna correlation, efficiency and bandwidth. While the first two aspects have received significant attention, antenna bandwidth with mutual coupling is a relatively uncharted territory. We show that while implementing a good matching network can drastically improve the system capacity for narrowband systems in the presence of strong mutual coupling, the same conclusions may not necessarily apply to wideband cases. To exemplify this, we carry out capacity simulations for an end-to-end MIMO system, where a recently proposed S-parameter approach is used in conjunction with the 3GPP-3GPP2 channel model to model realistic wideband channel and antenna effects at both transmit and receive ends.**

Keywords-MIMO system; mutual coupling; channel capacity

I. INTRODUCTION

A MIMO (multiple-input-multiple-output) system makes simultaneous use of multiple antennas at both the transmitter and receiver ends to exploit the spatial channel for increasing the capacity [1], [2]. The advantages of MIMO systems are well known in the meantime, and have led to a large number of publications, as well as the emergence of commercial systems based on this technology.

Correlation of the signals at the different antenna elements can considerably decrease the capacity of a MIMO system [3]. Such correlation occurs particularly for compact MIMO systems, where the separation between the antennas is small; this effect has been investigated extensively. In addition, with a small separation, the effect of mutual coupling between the antennas becomes important.

Refs. [4]-[12] investigated the impact of this effect on antenna correlation and MIMO capacity. However, these investigations present conflicting results on the impact of mutual coupling on channel capacity. One view claims that mutual coupling is beneficial to capacity [4], while another claims that it degrades the capacity [5], [6], [7]. There are also those who pointed out that mutual coupling can be beneficial to capacity performance, but only for certain cases (e.g. a range of antenna separations) [8], [9]. Some related works, such as [10],

[11] and [12], study the impact of mutual coupling on capacity without making direct comparisons with the no- coupling case.

Of these contributions, it appears that [9] and [12] present the most comprehensive studies to date. Interestingly, both papers independently proposed the use of S-parameter representation to model an entire narrowband communication system. One major advantage of their end-to-end approach is that both the signal correlation and the efficiency of the antenna system are accurately modeled. Both papers demonstrate that the proper inclusion of antenna efficiency results in smaller capacity, particularly at small antenna spacing. But while [9] focused on the impact of mutual coupling for two parallel dipoles with different terminations, [12] studied two different MIMO systems (multiplexing and beamforming) and the impact of having different antenna array configurations (though also dipoles) using only the self-impedance match.

In this contribution, we extend the approach to study *wideband* systems. Bandwidth becomes an important consideration since mutual coupling can severely reduce the bandwidth of the antenna system as compared to the single-antenna case. To our knowledge, little is known about the impact of different terminations (or matching) on the antenna bandwidth, in the case of multiple antennas with mutual coupling, though [13] has inferred that good matching will degrade the bandwidth performance.

We begin this paper with an introduction to the system model, the S-parameter modeling approach and the performance measures in Sections II, III and IV. We then summarize the impact of mutual coupling on three different measures influencing capacity: correlation, efficiency, and bandwidth. We show how the different matching networks behave under these measures according to the extent of their matching to the self and mutual impedances of the antenna system. Finally, we evaluate the impact of mutual coupling on MIMO capacity with respect to the 3GPP-3GPP2 MIMO channel model [14] and different matching conditions. We compare the capacity performance between the narrowband and wideband cases.

II. MIMO SYSTEM MODEL

Figure 1 presents the simplified model of a 2×2 MIMO system. We assume downlink transmission, though the model is equally applicable on the uplink. For the sake of convenience,

we do not explicitly show the frequency dependence of system parameters, except in Section IV-D.
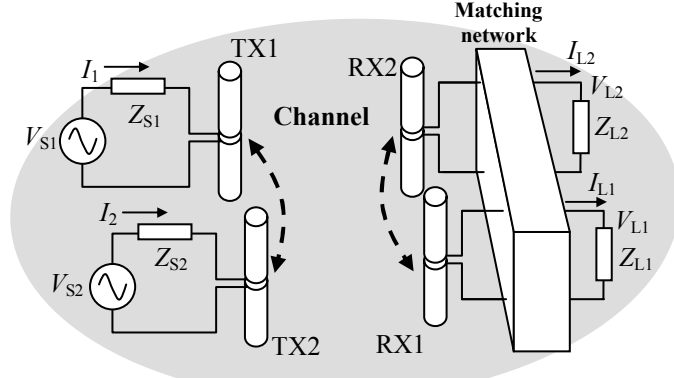

Figure 1. A 2×2 MIMO communication system: Transmit subsystem, propagation channel and receive subsystem. Dashed line with arrowheads represent coupling between antennas.

A. Transmit Subsystem

In the transmit subsystem or base station (BS), a voltage source with a source impedance Z_{Si} is connected across the feed of each dipole antenna. The two-antenna configuration with separation distance d can be represented by a 2×2 impedance matrix $\mathbf{Z}_{TT}$, where for identical dipoles and $Z_{ij} = [\mathbf{Z}_{TT}]_{ij}$, $Z_{11} = Z_{22}$ and $Z_{12} = Z_{21}$. Due to its single-mode operation [15], the radiated field per unit feed current of the jth antenna may be deduced from $\mathbf{Z}_{TT}$ and its open-circuit field $e_j^T(\theta)$. $e_j^T(\theta)$ is obtained using the MoM implementation of [16].

B. Propagation Channel

The 3GPP-3GPP2 channel model [14] is used for the capacity simulations. It provides a realistic channel response in the spatial and delay domains. Previous works, e.g. [8], [9], and [12] have only studied narrowband systems.

C. Receive Subsystem

The receive subsystem or mobile station (MS) is nearly identical to the transmit subsystem (with load impedance Z_{Li} instead of Z_{Si}) except for the absence of the voltage sources and the presence of a 2×2 matching network at the antenna termination. Unlike the BS, the matching network is important for the MS due to its power limitation and increasing compactness. As with the BS, the induced current per incident field of the ith antenna can be deduced from the impedance matrix of the receive antennas $\mathbf{Z}_{RR}$ and induced current for the open-circuit case $E_i^R(\theta)$, both of which are obtained from [16].

III. S-PARAMETER MODELING

Although the Z-parameter representation is often used to represent the communication blocks in Fig. 1, e.g. [17], it is convenient to use the S-parameter representation for capacity calculations [9]. The Z- and S-parameter matrices are related by the transformation $\mathbf{S} = (\mathbf{Z} + Z_0\mathbf{I})^{-1}(\mathbf{Z} - Z_0\mathbf{I}) = \Im_{Z-S}(\mathbf{Z})$, where Z_0 is the (real-valued) characteristic (or reference) impedance. The combined S-matrix of the transmit antennas, channel and receive antennas is given by [9]

$$\mathbf{S}_H = \begin{bmatrix} \mathbf{S}_{TT} & \mathbf{S}_{RT} \\ \mathbf{S}_{TR} & \mathbf{S}_{RR} \end{bmatrix} \qquad (1)$$

where $\mathbf{S}_{TT}$ and $\mathbf{S}_{RR}$ are S-parameter equivalents of $\mathbf{Z}_{TT}$ and $\mathbf{Z}_{RR}$. As in [9] and [12], we assume negligible backscattering from the receive antennas to the transmit antennas, i.e. $\mathbf{S}_{TR} = \mathbf{0}$. $\mathbf{S}_{RT}$ denotes the transmission characteristics from TX to RX antenna, and is given by [9]

$$\mathbf{S}_{RT} = \left(\mathbf{I} + \frac{\mathbf{Z}_{RR}}{\mathbf{Z}_0} \right)^{-1} \frac{\mathbf{Z}_{RT}}{\mathbf{Z}_0} (\mathbf{I} - \mathbf{S}_{TT}) \qquad (2)$$

where $\quad [\mathbf{Z}_{RT}]_{ij} = \sum_{n=1}^{N_p} E_i^R(\theta_n^{\text{DoA}}) \beta_n e_j^T(\theta_n^{\text{DoD}}),$ (3)

$e_j^T(\theta)$ and $E_i^R(\theta)$ are defined earlier, θ_n^{DoD}, θ_n^{DoA}, β_n are respectively the direction-of-departure, direction-of-arrival and complex gain of the nth path. For the wideband case, the channel response can be obtained over a range of frequency bins, each of which is shaped by the antenna response over those frequencies. The matching network is represented by [9]

$$\mathbf{S}_M = \begin{bmatrix} \mathbf{S}_{11} & \mathbf{S}_{12} \\ \mathbf{S}_{21} & \mathbf{S}_{22} \end{bmatrix} \qquad (4)$$

Some common matching networks found in literature, as well as a new type of matching, are given in the following.

A. Characteristic Impedance Match

This is when antennas are terminated with the load Z_0. In other words, there is no matching network, i.e. $\mathbf{S}_{11} = \mathbf{S}_{22} = \mathbf{0}$.

B. Self Impedance Match

As opposed to $\mathbf{S}_{11} = \text{diag}\{\mathbf{S}_{RR}^*\}$ of [9] and [18], we follow the more common definition, i.e. $\mathbf{S}_{11} = \Im_{Z-S}\left((\text{diag}\{\mathbf{Z}_{RR}\})^* \right)$, where $\text{diag}\{\bullet\}$ diagonalizes the operand.

C. Multiport Conjugate (MC) Match

The so-called multiport conjugate match requires one side of the matching network to be *conjugate-matched* to the antenna and the other side to the load [9], i.e. $\mathbf{S}_{11} = \mathbf{S}_{RR}^H$ and $\mathbf{S}_{22} = \mathbf{S}_L^H$, where $(\bullet)^H$ denotes conjugate-transpose. In our case of Z_0 termination, $\mathbf{S}_{22} = \mathbf{0}$. A practical implementation of the MC match [9] for the two-dipole case has been demonstrated in a paper [19] using a matching network consisting of transmission lines and open-circuited stub. Since the two papers appeared at around the same time, the authors of [19] appear to be unaware of [9], and presented the matching network in the context of jointly optimizing for minimum envelope correlation and maximum antenna system efficiency.

Of the three above cases, only the MC match explicitly accounts for mutual coupling. For lossless network, $\mathbf{S}_{12}$ and $\mathbf{S}_{21}$ of these four cases are simply found from

$$\mathbf{S}_{11}^H \mathbf{S}_{11} + \mathbf{S}_{21}^H \mathbf{S}_{21} = \mathbf{I} \qquad (5)$$

$$\mathbf{S}_{12}^H \mathbf{S}_{12} + \mathbf{S}_{22}^H \mathbf{S}_{22} = \mathbf{I} \qquad (6)$$

Without loss of generality[1], we assume that

$$Z_{Si} = Z_{Li} = Z_0 = 50\Omega, \quad i = 1,2 \tag{7}$$

IV. PERFORMANCE MEASURES

A. Antenna Correlation

The calculation of antenna correlation with S-parameters for different types of termination (or matching) is given in [18]. The MC match is called the optimal Hermitian match in [18].

B. Matching Efficiency

Here we are concerned with the efficiency of the receive antenna chain, in terms of the power received at the antenna. This is a reciprocal concept to transmit efficiency, as opposed to the much discussed absorption efficiency, e.g. [22], which considers also power scattered by the antenna. The purpose is to investigate how much *received* power is reflected and re-radiated. The output reflection coefficient looking into the matching network from the termination side is given by [18]

$$\mathbf{\Gamma}_{out} = \mathbf{S}_{22} + \mathbf{S}_{21}\left(\mathbf{I} + \mathbf{S}_{RR}\mathbf{S}_{11}\right)^{-1}\mathbf{S}_{RR}\mathbf{S}_{12} = \begin{bmatrix} r_{11} & r_{12} \\ r_{21} & r_{22} \end{bmatrix}, \tag{8}$$

and the corresponding matching efficiency is defined as [19]

$$\rho_M = 1 - |r_{11}|^2 - |r_{12}|^2. \tag{9}$$

For perfect matching (i.e. MC match), $\mathbf{\Gamma}_{out} = \mathbf{0}$ and $\rho_M = 1$.

C. Bandwidth

For the 2×2 MIMO system, the antenna bandwidth differs from that of a single-antenna when mutual coupling effect becomes significant. To our knowledge, no standard definition has been given for a combined measure of bandwidth. Instead, we will illustrate the impact of capacity on bandwidth using plots of $|r_{11}|$ and $|r_{12}|$ in the next section.

D. Capacity

The channel capacity over a bandwidth B (in bits/s/Hz) is

$$C = \frac{1}{B}\int_B \log_2\left\{\det\left(\mathbf{I} + \frac{1}{\sigma_n^2}\mathbf{H}(f)\mathbf{Q}(f)\mathbf{H}^H(f)\right)\right\}df, \tag{10}$$

where

$$\mathbf{H}(f) = \mathbf{\Lambda}_D^{1/2}(f)\mathbf{\xi}_D^H(f)\mathbf{S}_{RT}(f), \tag{11}$$

and

$$Z_0\left(\mathbf{I} - \mathbf{S}_{RR}(f)\mathbf{S}_{11}^H(f)\right)^{-1} = \mathbf{\xi}_D(f)\mathbf{\Lambda}_D^{1/2}(f)\mathbf{\xi}_D^H(f), \tag{12}$$

and $\mathbf{Q}$ is the source covariance matrix and σ_n^2 is the noise (we assume noise power density constant over B). The total transmit power is $P_T = \int_B \text{tr}\left(\mathbf{Q}(f)\right)$. For equal power distribution over space and frequency, $\mathbf{Q}(f) = P_T/BN_t$ where N_t is the number of transmit antennas. The waterfilling solution is well known. In our capacity simulations we consider waterfilling over space for the narrowband case and joint waterfilling over

---

space and frequency for the wideband case [23].

V. NUMERICAL EXAMPLES AND SIMULATIONS

Here we use the model described in Sections II and III to analyze a 2×2 MIMO system. Half-wavelength ($\lambda/2$) electric dipole antennas of diameter $\lambda/400$ are approximated by thin strips of equal length and width of twice the diameter [16]. Although the dipole is relatively narrowband and uncommon in practice, its simplicity and well-studied behavior make it a popular reference case.

We design the matching network at the center frequency f_c of the system for each antenna separation d using transmission lines and open-circuited stubs, as shown in [19] and [21]. The frequency response of the network can then be calculated. We note that the $\mathbf{S}_{11} = \mathbf{S}_{RR}^H$ condition for MC match can only be approximated using the proposed procedure in [19] and thus $\mathbf{\Gamma}_{out} \approx \mathbf{0}$. The goodness of the approximation varies according to the optimized local solutions.

A. Antenna Correlation

It can be seen in Fig. 2 that for very small separations $d < 0.2\lambda$, the MC match results in the lowest antenna correlation, while the Z_0 match and the self impedance match have nearly the same performance.

One interesting observation is the result for the MC match differs from that in [9] over this separation range. This effect is due to the different thickness of the dipole. In [9], the dipole has a diameter of 0.02λ, and it is found that uneven current distributions around the antenna's circumference become significant when the separation is in the order of the thickness of the antenna, i.e. 0.02λ. At $d < 0.02\lambda$, the antennas are touching/merging and the results are no longer meaningful.

For our dipole of diameter $\lambda/400$, this effect is negligible in the considered range $d \in [0.01\lambda, 1.25\lambda]$. We confirmed the validity of the strip model (which does not model the uneven current distribution) by making comparisons with a cylinder approximation of the dipole using [16]. It was found that for thin dipoles of diameter $\lambda/400$, both models agree very well in the range $d \in [0.01\lambda, 1.25\lambda]$.

B. Matching Efficiency

Figure 3 summarizes the matching efficiency (9) of the different terminations. Since Z_0 does not match either the self or mutual impedance of the antenna, the Z_0 match gives the worst result. The perfect matching achieved by the MC match allows it to retain efficiency of 1, even for very close antenna spacing, while the (partially-matched) self impedance match has a performance between the two other cases.

For wideband systems, Figs. 4(a)-(c) show the matching efficiency for each of the four different matching terminations over both antenna separation and frequency. Except for the MC match of Fig. 4(c) at some antenna separations (partly due to goodness of the designed network), the efficiency measure does not vary significantly over frequency. It is obvious that the Z_0 match does not achieve efficiency of 1, even for larger antenna separations where mutual coupling is less severe, This is due to the mismatch between the self and Z_0 impedances.
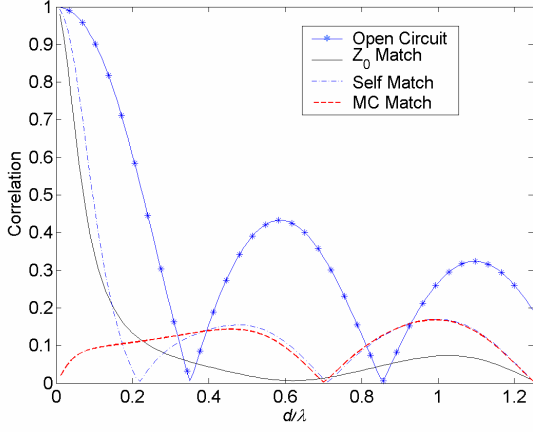
Figure 2. Antenna correlation at different antenna separations for different termination conditions.
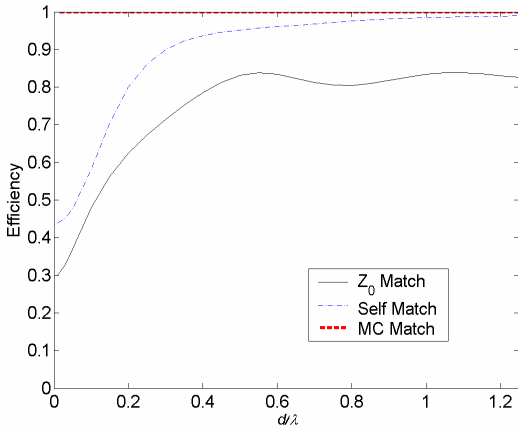

Figure 3. Radiation efficiency at different antenna separations for different termination conditions.
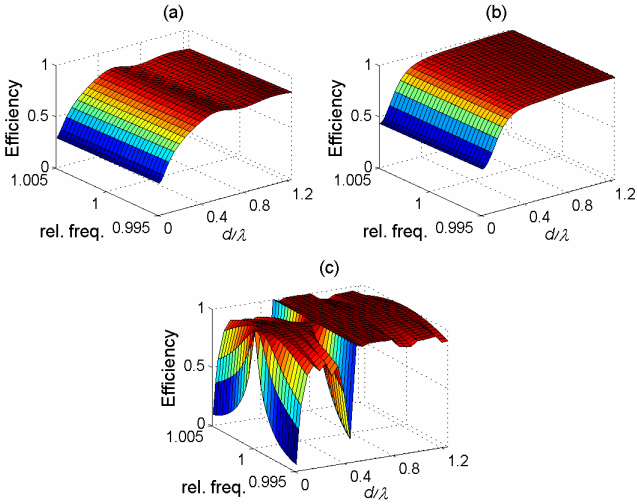

Figure 4. Matching efficiency at different antenna separations for different termination conditions: (a) Z_0 match, (b) Self match, and (c) MC match.

C. Antenna System Bandwidth

Figures 5 show the behaviors of $|r_{11}|$ and $|r_{12}|$ over frequency and antenna separation for different termination conditions. $|r_{11}|$ and $|r_{12}|$ in Fig. 5(a) and 5(b) have only small variations over the frequency domain. This is because a single dipole, though relatively narrowband, has a bandwidth of around 5-10% and this translates to 100-200 MHz at $f_c = 2$ GHz. On the other hand, $|r_{11}|$ and $|r_{12}|$ vary with d according to the self and mutual impedances (see e.g. Fig. 4 in [9]). In particular, $|r_{12}|$ becomes increasingly large at closer separation, due to the strong coupling into the adjacent circuit.

The use of self-impedance match clearly improves $|r_{11}|$, as compared to the Z_0 match (compare Fig. 5(a) and (c)). This is not surprising, as it matches the self-impedance of the dual-antenna system. However, no apparent improvement is seen in Fig. 5(d) for $|r_{12}|$, as mutual coupling is not matched.
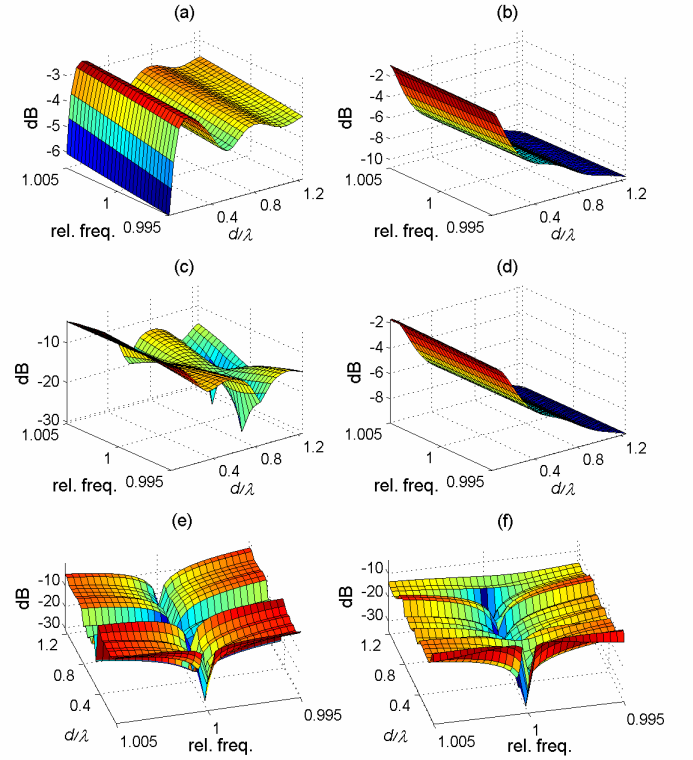

Figure 5. $|r_{11}|$ and $|r_{12}|$ over different antenna separations and frequency points for different terminations: (a) $|r_{11}|$ and (b) $|r_{12}|$ for Z_0 match, (c) $|r_{11}|$ and (d) $|r_{12}|$ for self impedance match, (e) $|r_{11}|$ and (f) $|r_{12}|$ for MC match.

It can be seen in Figs. 5(e) and (f) that the MC match appears to present a more attractive matching solution, as it has a fairly even performance for $|r_{11}|$ *and* $|r_{12}|$. Unfortunately, it is nontrivial to obtain a well optimized solution using the procedure in [19] and the optimized point is non-robust to small changes in the lengths of the circuit elements used. We also note that the bandwidth of the antenna narrows at small antenna separations. This is also exemplified in the efficiency performance in Fig. 4(c). Arguably, better bandwidth performance can be achieved by a different implementation of

the MC match than that of [19]. For the single antenna case, the Bode-Fano criterion [21] defines an upper bound for achievable antenna bandwidth with any matching. However, such results are unavailable for multiple antennas.

D. Capacity Simulation

We perform the capacity analysis over the prescribed bandwidth of 5 MHz for the 3GPP-3GPP2 channel model with $f_c = 2$ GHz. We focus on the *Urban Microcell* scenario with one stationary MS and one BS. The main channel parameters are summarized in Table 1 [14], where $U(a,b)$ is a uniform distribution over (a,b) and $\eta(0,\sigma^2)$ a zero-mean Gaussian distribution with variance σ^2. Lognormal shadow fading and path loss are not modeled, as they are irrelevant to the present study. We consider only the non line-of-sight case.

Channel Scenario	Urban Micro
Number of paths (N)	6
Number of sub-paths (M) per-path	20
Mean AS at BS	NLOS: 19°
Per-path AS at BS (Fixed)	5° (LOS and NLOS)
BS per-path AoD Distribution standard distribution	$U(-40°, 40°)$
Mean AS at MS	68°
Per-path AS at MS (fixed)	35°
MS Per-path AoA Distribution	$\eta(0,\sigma_{AoA}^2)$
Mean total RMS Delay Spread	0.251 μs
Distribution for path delays	$U(0, 1.2$ μs$)$

Table 1. Urban Microcell parameters of 3GPP-3GPP2 channel model.

The mean capacity is obtained for 5000 realizations of the channel. For each realization, the MS is at a fixed distance from the BS, but its orientation with respect to the BS is randomly generated from $U(0,360°)$. The antenna spacing at the BS is set at $d = 0.5\lambda$, while for the MS, $d \in [0.01\lambda, 1.25\lambda]$. We assume that the receive antennas are in the far field of the transmit antennas. As a benchmark, the no-coupling case for the Z_0 match is used to find the noise level (for a given P_T) to give 20 dB SNR for the single antenna case. The same P_T and noise level are then used for all mutual coupling cases. It should be noted that the self impedance of the antenna for the no-coupling case is the (fixed) input impedance of an isolated dipole. This approach is akin to that of [9], where the emphasis is on a fair comparison among the different matching conditions. Here we only consider the transmit power constraint $P_T \leq P_{max}$ for the *supplied power* of the voltage sources, while [9] also studied the modified waterfilling approach which enforces the constraint on the *radiated power*.

To investigate the impact of bandwidth on the results, we first consider the narrowband case in Fig. 6 (as in [9] and [12]), where only the mean capacity at the center frequency is calculated (waterfilling over space only). The capacity performance of the no-coupling (Z_0 match) case shares a similar trend to that in [9]. It is obvious that without a matching network, the capacity performance of Z_0 match with coupling degrades consistently over the given range of antenna separation. The self impedance match fairs better than the reference Z_0 match with no coupling, and only becomes worse

at smaller antenna separations $d < 0.1\lambda$. The poorer capacity performance at $d < 0.1\lambda$ is due to the severe effect of mutual coupling impairing both the antenna correlation and matching efficiency. The difference in the mean capacities between Z_0 match and self impedance match (and MC match) at larger separations is due to the loss of efficiency for the Z_0 match from not matching the termination to the self impedance of the antenna. The performance of the self impedance match and the MC match converges to each other at larger separations, due to the decreasing mutual coupling effect, which is not taken into account by the self impedance match. The good performance of the MC match at smaller antenna separations $d < 0.4\lambda$, as compared to other cases, can be understood from its low correlation and near 100% (or 1) matching efficiency. The slight dip in capacity at $d < 0.03\lambda$ is attributed to the difficulty in designing a good matching network using the optimization procedure of [19], as can be observed in Fig. 5(e) and (f).

In the wideband case of Fig. 7, we observe nearly identical trends to those in Fig. 6. This is because the bandwidth of 5 MHz is relatively narrow (0.25% of the center frequency), and the mismatch between the matching network and the antenna impedances is not yet severe. This is particularly the case for the MC match, which demonstrates the greatest variations in the frequency response at small antenna separations. Nevertheless, it can be seen by comparing Figs. 6 and 7 that the mean capacity of the MC match differs by 0.7 bits/s/Hz at $d = 0.01\lambda$. This is easily attributed to the "narrow valley" in Figs. 5(e) and (f).

VI. CONCLUSIONS

In this contribution, we investigated the impact of mutual coupling on capacity for compact MIMO systems. We found that for the case of wideband systems, the frequency dependence of the dipole antenna system can degrade the capacity performance at close antenna separation, as compared to the narrowband case. This is due to the frequency response of the matching network, which is not exactly matched to that of the antenna system over a finite bandwidth. Therefore, we conclude that, capacity performance in the presence of mutual coupling can differ between the narrowband and wideband cases.
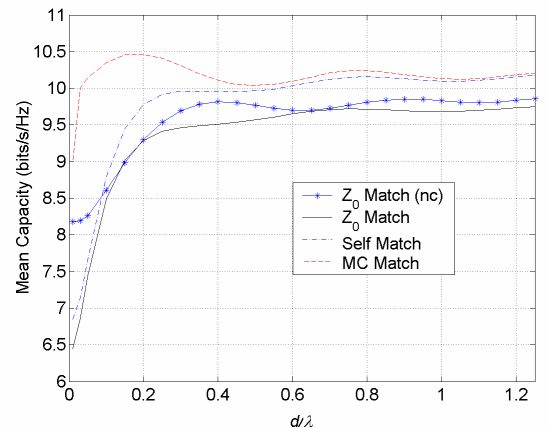

Figure 6. Mean capacities for different matching conditions at different receive antenna separations (Narrowband case).
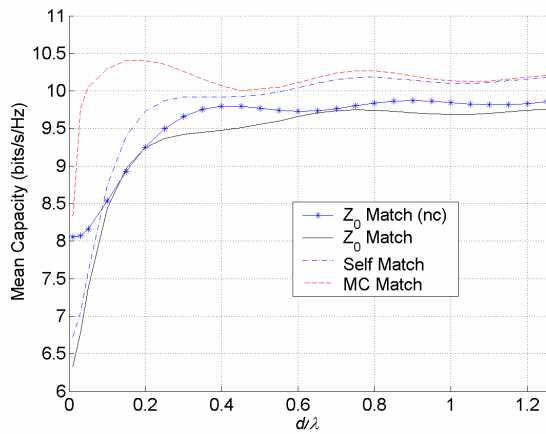
Figure 7. Mean capacities for different matching conditions at different receive antenna separations (Wideband case).

REFERENCES

[1] I. E. Telatar, "Capacity of multi-antenna Gaussian channels," *European Trans. Telecommun.*, vol. 10, pp. 585-595, 1999.

[2] G. J. Foschini and M. J. Gans, "On limits of wireless communications in a fading environment when using multiple antennas," *Wireless Personal Communications* (Kluwer Academic Publishers), vol. 6, pp. 311–335, Mar. 1998.

[3] D. S. Shiu, G. J. Foschini, M. J. Gan, J. M. Kahn, "Fading correlation and its effect on the capacity of multielement antenna systems," *IEEE Trans. Commun.*, vol. 48, pp. 502-513, Mar. 2000.

[4] T. Svantesson and A. Ranheim, "Mutual coupling effects on the capacity of multielement antenna systems," *Proc. IEEE ICASSP*, vol. 4, pp. 2485-2488, Salt Lake City, Utah, May 7-11, 2001.

[5] P. N. Fletcher, M. Dean, and A. R. Nix, "Mutual coupling in multi-element array antennas and its influence on MIMO channel capacity," *Electron. Lett.*, vol. 39, no. 4, pp. 342-344, 20th Feb. 2003.

[6] R. Janaswamy, "Effect of element mutual coupling on the capacity of fixed length linear arrays," *IEEE Antennas and Wireless Propagat. Lett.* , vol. 1, no. 8, pp. 157-160, 2002.

[7] M. K. Ozdemir, E. Arvas, and H. Arslan, "Dynamics of spatial correlation and implications on MIMO systems," *IEEE Commun. Mag.*, vol. 42, pp. S14-S19, Jun. 2003.

[8] B. Clerckx, D. Vanhoenacker-Janvier, C. Oestges, and L. Vanderdorpe, "Mutual coupling effects on the channel capacity and the space-time processing of MIMO communication systems," in *Proc. IEEE ICC*, vol. 4, pp. 2638-2642, Anchorage, Alaska, 11-15 May 2003.

[9] J. W. Wallace and M. A. Jensen, "Mutual coupling in MIMO wireless systems: a rigorous network theory analysis," *IEEE Trans. Wireless Commun.*, vol. 3, pp. 1317-1325, Jul. 2004.

[10] V. Jungnickel, V. Pohl, and C. von Helmolt, "Capacity of MIMO systems with closely spaced antennas," *IEEE Commun. Lett.*, vol. 7, no. 8, pp. 361-363, Aug. 2003.

[11] B. Lindmark, "Capacity of a 2 x 2 MIMO antenna system with mutual coupling losses," in *Proc. IEEE Antennas and Propagation Society International Symposium*, vol. 2, pp. 1720-1723, Monterey, CA, 20-25 Jun. 2004.

[12] C. Waldschmidt, S. Schulteis, and W. Wiesbeck, "Complete RF system model for analysis of compact MIMO arrays," *IEEE Trans Vehic. Technol.*, vol. 53, no. 3, pp. 579-586, May 2004.

[13] H. J. Chaloupka and X. Wang, "On the properties of small arrays with closely spaced antenna elements," in *Proc. IEEE Antennas and Propagation Society International Symposium*, vol. 3, pp. 2699-2702, Monterey, CA, 20-25 Jun. 2004.

[14] 3GPP-3GPP2 ad-hoc Spatial Channel Modeling Group, "MIMO channel model", v.6.0 Document 134, http://www.3gpp.org/ftp/tsg_ran/WG1_RL1/3GPP_3GP P2_SCM/.

[15] H. Steyskal and J. S. Herd, "Mutual coupling compensation in small array antennas," *IEEE Trans. Antennas Propagat.*, vol. 38, pp. 1971-1975, Dec. 1990.

[16] S. N. Makarov, Antenna and EM Modeling with MATLAB®, *Wiley-Interscience*, 2002.

[17] R. Vaughan and J. B. Andersen, *Channels, Propagation and Antennas for Mobile Communications*, The IEE, 2003.

[18] J. W. Wallace and M. A. Jensen, "Termination-dependent diversity performance of coupled antennas: Network theory analysis," *IEEE Trans. Antennas Propagat.*, vol. 52, pp. 98-105, Jan. 2004.

[19] S. Dossche, S. Blanch, and J. Romeu, "Optimum antenna matching to minimise signal correlation on a two-port antenna diversity system," *Electronic Lett.*, vol. 40, no. 19, pp. 1164-1165, 16 Sep. 2004.

[20] S. J. Orfanidis, *Electromagnetic Waves and Antennas*, http://www.ece.rutgers.edu/~orfanidi/ewa.

[21] D. M. Pozar, *Microwave Engineering*, New York: Wiley, 1998.

[22] D. Pozar, "Scattered and absorbed powers in receiving antennas," *IEEE Antennas Propagat. Mag.*, vol. 46, no. 1, pp. 144-145, Feb. 2004.

[23] P. Almers, R. Tufvesson, O. Edfors, and A. F. Molisch, "Measured capacity gain using waterfilling in frequency selective MIMO channels," in *Proc. IEEE PIMRC*, vol. 3, pp. 1347-1351, Lisbon, Portugal, 15-18 Sep. 2002.